

Error performance analysis of different modulations over TWDP fading channel

Almir Maric, *Member, IEEE*, and Pamela Njemcevic, *Member, IEEE*

Abstract

Two-wave with diffuse power (TWDP) is one of the most promising distribution for description of a small-scale fading in the emerging mmWave band. However, traditional error performance analysis in these channels faces two fundamental issues. It is mostly based on conventional TWDP parameterization which is not in accordance with the model's underlying physical mechanisms and which hinders accurate observation of the impact of a model parameters on a system's performance metrics. In addition, the existing average bit/symbol error probability (ABEP/ASEP) expressions for most modulations and diversity schemes are available as approximations, which are accurate only for specific combinations of TWDP parameters. Accordingly, in this paper, the exact ASEP expressions are derived for M-ary rectangular quadrature amplitude modulation (RQAM) with coherent detection and for M-ary DPSK modulation, and are given in terms of physically justified parameters. Besides, in order to relax computational complexity of proposed exact ASEPs in high signal-to-noise ratio (SNR) region, their asymptotic counterparts are derived as the simple closed-form expressions, matching the exact ones for $\text{SNR} > 30\text{dB}$. Results are verified by Monte-Carlo simulation.

Index Terms

TWDP fading channel, ASEP, RQAM, DPSK.

I. INTRODUCTION

TWDP is a small-scale fading model, introduced by Durgin *et al.* for modeling Rician, Rayleigh and hyper-Rayleigh fading conditions [1]. It assumes that received signal's complex envelope is composed of two strong specular components and many weak diffuse components.

A. Maric and P. Njemcevic are with the Department of Telecommunications, Faculty of Electrical Engineering, University of Sarajevo, Sarajevo, Bosnia and Herzegovina.

e-mail: almir.maric@etf.unsa.ba;

It is empirically shown that such a signal occurs in 5G networks, where mmWave band and directional antennas are employed [2]–[4], as well as in wireless sensor networks deployed in cavity environments such as airplanes, buses, etc. [5], [6].

Although applicable for modeling of received signals in different emerging technologies, TWDP model from its inception has been facing two major issues. First, initial TWDP probability density function (PDF) expressions are given in integral or approximate forms, which hinders the exact wireless system performance analysis in channels with TWDP fading [7]. Besides, conventional TWDP parameterization is shown to be inconsistent with model's underlying physical mechanisms, which complicates observation of the impact of the ratio between different signal components on a system's performance metrics [8].

Namely, the original TWDP envelope PDF [1, eq. (32)] is given in integral form, which couldn't be used for further mathematical manipulations. So, as a solution, Durgin *et al.* proposed the closed-form approximation of TWDP envelope's PDF [1, eq. (17)], used in many papers to evaluate error performance of wireless communication systems with the single- and multi-antenna reception. Accordingly, average symbol/bit error probabilities are derived for different modulations and diversity schemes, either by averaging conditional BEP/SEP in channel with additive white Gaussian noise (AWGN) over the approximate TWDP PDF [1, eq. (17)] (PDF approach), or based on the approximate moment generation function (MGF) [9, eq. (11)] also derived from [1, eq. (17)] (MGF approach). Comprehensive overview of these results, classified according to derivation approach and according to treated modulation and diversity techniques, is given within the first two columns of Table I.

Overviewed papers have obviously provided the first analytical insight in ABEP/ASEP for channels with TWDP fading in a number of scenarios [7]. However, obtained results are approximations and their accuracy is known to degrade as the power of two specular components become stronger in respect to the power of diffuse components, while simultaneously two specular components become similar in strength [1]. Besides, they are all based on conventional parameterization, which disables clear observation of the effect of different ratios between specular components on ABEP/ASEP values [8].

Step forward in error performance analysis over the TWDP fading channels had been made in [7], by derivation of a closed-form TWDP MGF expression [7, eq. (25)]. However, although exact, it is shown that proposed MGF expression is not appropriate for mathematical manipulations.

Table I: An overview of available average error probability expressions for different modulation and diversity techniques in TWDP channel

| Modulation (coherent detection) | | <i>Approx. expressions</i> | | <i>Exact expressions</i> |
|---------------------------------------|--------------|----------------------------|--------------|--------------------------|
| | | PDF approach | MGF approach | |
| BPSK | no diversity | [10] | | [8] |
| | L-branch SC | [11] | | |
| | L-branch EGC | [12] | | |
| | L-branch MRC | [13] | [9] | |
| M-ary PSK | no diversity | [14] | | [8] |
| | 2-branch SC | | [15] | |
| | L-branch MRC | [13] | | |
| M-ary SQAM | no diversity | | [16] | |
| | L-branch MRC | [13] | | |
| M-ary RQAM | no diversity | [17] | [16] | |
| | 2-branch SC | | [15] | |
| | L-branch SC | [18] | | |
| | L-branch MRC | | [19] | |
| Modulation (noncoherent detection) | | <i>Approx. expressions</i> | | <i>Exact expressions</i> |
| | | PDF approach | MGF approach | |
| BFSK | no diversity | | | [7] |
| | 2-branch SSC | [20] | [21] | |
| | L-branch SC | [11] | | |
| | L-branch EGC | | [22] | |
| | L-branch MRC | [13] | | |
| M-ary FSK | no diversity | | | [7] |
| | 2-branch SSC | [23] | | |
| | L-branch EGC | | | [24] |
| DBPSK | no diversity | | | [25] |
| | L-branch SC | [11] | | |
| | L-branch EGC | | [22] | |
| M-ary DPSK | L-branch MRC | [13] | | |

Accordingly, it is used only for derivation of the exact error probability of binary DPSK [7], [25] and noncoherent M-ary frequency shift keying (FSK) modulations without diversity [7] and with the equal gain combining (EGC) reception [24], also in terms of conventional TWDP parameters.

However, improved TWDP parameterization that is in accordance with model's underlying physical mechanisms is recently proposed in [8]. Besides, the alternative form of the exact MGF [8, eq. (22)] is also derived based on the exact PDF [26, eq. (6)], and expressed in terms of improved parameters. It is shown that proposed form of MGF is suitable for mathematical manipulations and demonstratively, it is used to derive the exact ASEP for M-ary PSK system with the single-antenna coherent detection [8].

So, despite the sporadic breakthroughs in TWDP error performance analysis, the exact error performance characterization which allows accurate observation of the impact of model parameters on a system's performance metrics, for most modulation and diversity schemes in TWDP channels, remains an open issue [7].

Accordingly, in this paper the exact ASEP expression for a generic, coherently detected M-ary RQAM system is derived and used for derivation of the exact ASEP for M-ary SQAM and M-ary amplitude shift keying (ASK), as well as for binary and quadrature PSK modulations, all in terms of physically justified TWDP parameters. The exact ASEP expression for M-ary DPSK modulated signal is also derived. The error performance of all considered modulations are then compared, revealing superiority of SQAM modulation and explaining reason for its extensive applicability in 5G and other networks in which multipath fading can be best described using TWDP model. In addition, for all considered modulations, high SNR asymptotic ASEPs are also derived as a simple closed-form expressions, enabling us to relax computational complexity of their exact counterparts in high SNR region.

The remainder of the paper is structured as follows: In Section II, TWDP channel model is presented. In Section III, the exact and asymptotic ASEP expressions for M-ary modulations with coherent and differential detection are derived. Results are verified in Section IV in terms of Monte-Carlo simulation. Conclusion is provided in Section V.

II. TWDP FADING MODEL

TWDP fading model, introduced in [1], is useful for modeling many practical wireless communication systems. It assumes that in the frequency nonselective slow fading channel, the complex envelope

$r(t)$ of the received signal is composed of two strong specular components $v_1(t)$ and $v_2(t)$ and many low-power diffuse components treated as a random process $n(t)$. Thus, $r(t)$ can be expressed as:

$$\begin{aligned} r(t) &= v_1(t) + v_2(t) + n(t) \\ &= V_1 \exp(j\Phi_1) + V_2 \exp(j\Phi_2) + n(t) \end{aligned} \quad (1)$$

In (1) specular components are assumed to have constant magnitudes V_1 and V_2 and uniformly distributed phases Φ_1 and Φ_2 in $[0, 2\pi)$, while diffuse components are treated as a complex zero-mean Gaussian random process $n(t)$ with the average power $2\sigma^2$. Consequently, the average power of $r(t)$ equals to $\Omega = V_1^2 + V_2^2 + 2\sigma^2$. Besides the average power Ω , two additional parameters K and Δ , defined in [1] as $K = (V_1^2 + V_2^2)/(2\sigma^2)$ and $\Delta = V_1V_2/(V_1^2 + V_2^2)$ respectively, are traditionally used for TWDP model description. However, it is shown in [8] that conventional Δ -based parameterization is not in accordance with model's underlying physical mechanisms. Consequently, its usage hinders accurate observation of the impact of the ratio between specular components on a system's performance metrics [8] and causes anomalies related to the estimation of these parameters [27]. To overcome the issues, improved TWDP parameterization, based on physically justified parameters K and Γ is introduced in [8]:

$$K = \frac{V_1^2 + V_2^2}{2\sigma^2}, \quad \Gamma = \frac{V_2}{V_1} \quad (2)$$

where K reflects the ratio between the powers of specular and diffuse components and Γ reflects the ratio between magnitudes of two specular components. Since it is shown that no anomalies related to the observation of the impact of a model parameters on ASEP [8] and to parameter estimation [27] can be observed when using improved parameters, parameterization based on K and Γ is used for description of TWDP fading in the remainder of this paper.

So, considering adopted parameterization and the overall model's assumptions, TWDP fading is properly described by its envelope PDF recently obtained in [8] based on [26], as the exact infinite-series expression:

$$\begin{aligned} f_R(r) &= \frac{r}{\sigma^2} \exp\left(-\frac{r^2}{2\sigma^2} - K\right) \sum_{m=0}^{\infty} \varepsilon_m (-1)^m I_m \left(2r \sqrt{\frac{K}{2\sigma^2} \frac{1}{1 + \Gamma^2}}\right) \\ &\quad \times I_m \left(2r \sqrt{\frac{K}{2\sigma^2} \frac{\Gamma^2}{1 + \Gamma^2}}\right) I_m \left(2K \frac{\Gamma}{1 + \Gamma^2}\right) \end{aligned} \quad (3)$$

where $\varepsilon_0 = 1$, $\varepsilon_m = 2$ for $m \geq 1$ and $I_\nu(\cdot)$ is a modified ν -th order Bessel function of the first kind. That expression is then used to derive the alternative form of the exact MGF of the SNR, given as [8]:

$$\mathcal{M}_\gamma(s) = \frac{1+K}{1+K-s\gamma_0} \sum_{m=0}^{\infty} \frac{1}{m!} \left(\frac{K}{1+\Gamma^2} \right)^m \times \left(\frac{\gamma_0 s}{1+K-s\gamma_0} \right)^m {}_2F_1(-m, -m; 1; \Gamma^2) \quad (4)$$

where $\gamma_0 = 2\sigma^2(1+K)\frac{T_s}{N_0}$ is the average SNR, T_s denotes symbol time, $N_0/2$ is the power spectral density of the white Gaussian noise and ${}_2F_1(\cdot, \cdot; \cdot; \cdot)$ is the Gaussian hypergeometric function.

It is shown in [8] that the alternative form of the MGF given by (4) can be reduced to the form of the MGF proposed in [7]. However, according to [8], this alternative form is much more suitable for mathematical manipulations. Since it is also given in terms of physically justified parameters, (4) is used as a basis for ASEP derivations in following section.

III. ERROR PROBABILITY PERFORMANCE ANALYSIS OVER TWDP CHANNELS

In wireless communication systems, accurate and tractable analysis of different system performance metrics is of profound significance for network planning and reliable transceiver design. Among these metrics, symbol error probability is one of the most important, since it enables us to quantify performance of systems with different modulations, when they are subjected to various TWDP fading conditions [17]. However, according to the overview provided in Section I, it is obvious that in considered channel, ABEP/ASEPs for most modulations are available only as approximate expressions given in term of nonphysical parameters, with the accuracy limited by the accuracy of employed approximate PDF expression.

A. Exact average symbol error probability expressions

According to the overview provided in Section I, the exact ASEP expressions in TWDP fading channels are available only for noncoherent M-ary FSK and differential BPSK modulations, as well as for M-ary PSK with a single-antenna coherent detection, while for all other modulations and diversity schemes, the exact expressions are missing. In additions, only the exact M-ary PSK ASEP is given in terms of parameters K and Γ . Accordingly, the following section closes the gap, by providing the exact ASEP expressions for remaining most popular M-ary modulation schemes in systems with the single-antenna reception, given in terms of physically justified K and Γ .

1) *M*-ary RQAM: The general order rectangular QAM is equivalent to two independent pulse amplitude modulation (PAM) signals (M_I -PAM in-phase and M_Q -PAM quadrature signals) [17]. Accordingly, the integral M-ary RQAM ASEP with the order of modulation $M = M_I \times M_Q$, can be expressed as [28]:

$$P_s^{RQAM}(\gamma_0) = a_I \int_0^{\frac{\pi}{2}} \mathcal{M}_\gamma \left(\frac{A_I^2}{2 \sin^2 \theta} \right) d\theta + a_Q \int_0^{\frac{\pi}{2}} \mathcal{M}_\gamma \left(\frac{A_Q^2}{2 \sin^2 \theta} \right) d\theta - \frac{\pi}{2} a_I a_Q \int_0^{\frac{\pi}{2} - \tan^{-1} \frac{A_Q}{A_I}} \mathcal{M}_\gamma \left(\frac{A_I^2}{2 \sin^2 \theta} \right) d\theta - \frac{\pi}{2} a_I a_Q \int_0^{\tan^{-1} \frac{A_Q}{A_I}} \mathcal{M}_\gamma \left(\frac{A_Q^2}{2 \sin^2 \theta} \right) d\theta \quad (5)$$

where

$$A_I = \sqrt{\frac{6}{(M_I^2 - 1) + \beta^2(M_Q^2 - 1)}}, \quad a_I = \frac{2}{\pi} \frac{M_I - 1}{M_I} \\ A_Q = \beta A_I, \quad a_Q = \frac{2}{\pi} \frac{M_Q - 1}{M_Q}$$

while β represents the ratio between quadrature and in-phase decision distances, i.e. $\beta = d_Q/d_I$.

So, after inserting (4) in (5), the exact ASEP of M-ary RQAM can be expressed as:

$$P_s^{RQAM}(\gamma_0) = \sum_{m=0}^{\infty} \left(\frac{K}{1 + \Gamma^2} \right)^m {}_2F_1(-m, -m; 1; \Gamma^2) \times \frac{1}{m!} \left[a_I \mathcal{I} \left(\frac{\gamma_0}{1 + K}, A_I, \frac{\pi}{2} \right) + a_Q \mathcal{I} \left(\frac{\gamma_0}{1 + K}, A_Q, \frac{\pi}{2} \right) - \frac{\pi}{2} a_I a_Q \mathcal{I} \left(\frac{\gamma_0}{1 + K}, A_I, \frac{\pi}{2} - \tan^{-1} \frac{A_Q}{A_I} \right) - \frac{\pi}{2} a_I a_Q \mathcal{I} \left(\frac{\gamma_0}{1 + K}, A_Q, \tan^{-1} \frac{A_Q}{A_I} \right) \right] \quad (6)$$

where $\mathcal{I}(\cdot, \cdot, \cdot)$ is defined as:

$$\mathcal{I}(a, A, \vartheta) = \int_0^{\vartheta} \frac{1}{1 - as} \left(\frac{as}{1 - as} \right)^m d\theta \Big|_{s=\frac{A^2}{2 \sin^2 \theta}} \quad (7)$$

Integral in (7) can be solved in terms of Appell's hypergeometric function $F_1(\cdot; \cdot, \cdot; \cdot; \cdot, \cdot)$ as:

$$\mathcal{I}(a, A, \vartheta) = (-1)^{m+1} \frac{2 \sin^3 \vartheta}{3 a A^2} \times F_1 \left(\frac{3}{2}; m + 1, \frac{1}{2}; \frac{5}{2}; \frac{2 \sin^2 \vartheta}{a A^2}, \sin^2 \vartheta \right) \quad (8)$$

with special cases:

$$\mathcal{I}(a, A, \frac{\pi}{2}) = (-1)^{m+1} \frac{\pi}{2 a A^2} {}_2F_1 \left(\frac{3}{2}; m + 1; 2; \frac{2}{a A^2} \right) \\ \mathcal{I}(a, A, \tan^{-1} \phi) = (-1)^{m+1} \frac{2}{3 a A^2} \left(\frac{\phi^2}{1 + \phi^2} \right)^{\frac{3}{2}} \times F_1 \left(\frac{3}{2}; m + 1, \frac{1}{2}; \frac{5}{2}; \frac{2}{a A^2} \frac{\phi^2}{1 + \phi^2}, \frac{\phi^2}{1 + \phi^2} \right)$$

$$\mathcal{I}(a, A, \frac{\pi}{2} - \tan^{-1} \phi) = (-1)^{m+1} \frac{2}{3aA^2} \left(\frac{1}{1 + \phi^2} \right)^{\frac{3}{2}} \times F_1 \left(\frac{3}{2}; m+1, \frac{1}{2}; \frac{5}{2}; \frac{2}{aA^2} \frac{1}{1 + \phi^2}, \frac{1}{1 + \phi^2} \right)$$

Considering the above given integral solution, the exact ASEP of a single-branch M-ary RQAM receiver is finally obtained as the exact expression, given by (13) in Table III.

2) *M-ary SQAM, M-ary ASK, QPSK and BPSK*: Rectangular QAM represents a generic modulation scheme since it includes SQAM, ASK, quadrature PSK and binary PSK schemes as its special cases. Accordingly, ASEP expressions for listed modulations can be obtained from (13) by employing specific values of RQAM parameters for each considered modulation (see Table II). Accordingly, ASEP for M-ary SQAM, M-ary ASK, QPSK and BPSK are listed in Table III and labeled by (14) - (17), respectively. It is also note worthy that the derived ASEPs for quadrature and binary PSK are exactly the same as the corresponding expressions obtained from M-ary PSK ASEP [8, eq. (28)] for $M = 4$ and $M = 2$ and accordingly, results based on these expressions are not going to be further elaborated.

It is also important to emphasize that among given results, those related to SQAM are of upmost importance, since SQAM presents a preferred modulation scheme in the emerging 5G networks due to its high bandwidth efficiency and implementation simplicity [16].

3) *M-ary DPSK*: In order to derive the exact M-ary DPSK ASEP, lets start from its integral counterpart, given in [7] as:

$$P_s^{DPSK} = \frac{1}{\pi} \int_0^{(1-\frac{1}{M})\pi} \mathcal{M}_\gamma \left(\frac{-\sin^2 \frac{\pi}{M}}{1 + \cos \frac{\pi}{M} \cos \theta} \right) d\theta \quad (9)$$

which can be, after inserting (4) in (9) and some manipulations, expressed as:

$$P_s^{DPSK}(\gamma_0) = \sum_{m=0}^{\infty} \frac{1}{m!} \left(\frac{K}{1 + \Gamma^2} \right)^m \times {}_2F_1(-m, -m; 1; \Gamma^2) (\mathcal{I}_m + \mathcal{I}_{m+1}) \quad (10)$$

Table II: M-ary RQAM: Special cases

| Modulation | RQAM parameters | | | | β |
|------------|-----------------|------------|--------------------------|--------------------------|---------|
| | M_I | M_Q | A_I | A_Q | |
| M-ary SQAM | \sqrt{M} | \sqrt{M} | $\sqrt{\frac{3}{M-1}}$ | $\sqrt{\frac{3}{M-1}}$ | 1 |
| M-ary ASK | M | 1 | $\sqrt{\frac{6}{M^2-1}}$ | $\sqrt{\frac{6}{M^2-1}}$ | 1 |
| QPSK | 2 | 2 | 1 | 1 | 1 |
| BPSK | 2 | 1 | $\sqrt{2}$ | $\sqrt{2}$ | 1 |

where $\mathcal{I}_{(\cdot)}$ is defined as:

$$\mathcal{I}_m = -\frac{1}{\pi} \int_0^{(1-\frac{1}{M})\pi} \left(1 + \frac{1 + \cos \frac{\pi}{M} \cos \theta}{a(1 - \cos^2 \frac{\pi}{M})} \right)^{-m} d\theta \quad (11)$$

By using binomial formula and after some manipulations, \mathcal{I}_m can be solved as:

$$\begin{aligned} \mathcal{I}_m &= \sum_{p=0}^{\infty} \binom{-m}{p} \left(\frac{b - Ab}{A} \right)^p \left(\frac{A}{a - b^2} \right)^{m+p} \\ &\times \left(\frac{\Gamma \left[\frac{p+1}{2} \right]}{2\sqrt{\pi}\Gamma \left[\frac{p+2}{2} \right]} - \frac{(-b)^{p+1}}{\pi(p+1)} \right) \\ &\times {}_2F_1 \left(\frac{1}{2}, \frac{p+1}{2}; \frac{p+3}{2}; b^2 \right) \end{aligned} \quad (12)$$

where $A = \frac{\gamma_0(1-b^2)}{1+K+\gamma_0(1-b^2)}$, $b = \cos \frac{\pi}{M}$, $a = \frac{\gamma_0}{1+K}$ and $\Gamma[\cdot]$ is the Gamma function. Accordingly, the exact M-ary DPSK ASEP expression can be determined as (18), given in Table III.

It is important to emphasize that by using [8, eq. (23)] and by employing the relation between parameters Γ and Δ (i.e. $\frac{2\Gamma}{\Gamma^2+1} = \Delta$), expression (18) for $M = 2$ can be reduced to the exactly the same expressions as the one derived in [7] by directly solving integral (9) for the same value of M .

B. Asymptotic average symbol error probability expressions

To effectively analyze the influence of TWDP fading on the achievable error rate performance of considered modulation techniques, the corresponding concise asymptotic closed-form ASEP expressions in the high SNR region are also derived, enabling us to relax the computational complexity which occurs for large values of K . Despite its importance, to the best of authors' knowledge, the asymptotic analysis is available only for BPSK [8], [29] and DBPSK [7] modulations with no diversity, while for all other modulation techniques these expression are missing.

1) *M-ary RQAM and its derivatives*: So, considering that $F_1(a; b_1, b_2; c; z_1, z) \sim {}_2F_1(a, b_1; c; z_1)$ and ${}_2F_1(a, b; c; z) \sim 1$ when $z \rightarrow 0$, equation (13) for large values of γ_0 can be expressed as (19), which represents the simple, closed-form asymptotic RQAM ASEP expression. By inserting the appropriate values of M_I , M_Q , A_I and A_Q in (19) given by Table II, the closed-form asymptotic ASEP expressions are also obtained for M-ary SQAM, M-ary ASK, QPSK and BPSK, and are given by (20) - (23), respectively (see Table IV).

Table III: Exact ASEP expressions

| Modulation | ASEP |
|---------------|--|
| M-ary RQAM | $P_s^{RQAM}(\gamma_0) = \frac{2}{\pi} \frac{1+K}{\gamma_0} \sum_{m=0}^{\infty} \frac{(-1)^{m+1}}{m!} \left(\frac{K}{1+\Gamma^2} \right)^m {}_2F_1(-m, -m; 1; \Gamma^2) \quad (13)$ $\times \left\{ \frac{2(M_I - 1)(M_Q - 1)}{3M_I M_Q (A_I^2 + A_Q^2)^{3/2}} \left[A_I F_1 \left(\frac{3}{2}; \frac{1}{2}, m+1; \frac{5}{2}; \frac{A_I^2}{A_I^2 + A_Q^2}, -\frac{2(K+1)}{(A_I^2 + A_Q^2)\gamma_0} \right) \right. \right.$ $\left. + A_Q F_1 \left(\frac{3}{2}; \frac{1}{2}, m+1; \frac{5}{2}; \frac{A_Q^2}{A_I^2 + A_Q^2}, -\frac{2(K+1)}{(A_I^2 + A_Q^2)\gamma_0} \right) \right] - \frac{\pi}{2A_I^2} \frac{M_I - 1}{M_I}$ $\times {}_2F_1 \left(\frac{3}{2}, m+1; 2; -\frac{2(K+1)}{A_I^2 \gamma_0} \right) + \frac{\pi}{2A_Q^2} \frac{M_Q - 1}{M_Q} {}_2F_1 \left(\frac{3}{2}, m+1; 2; -\frac{2(K+1)}{A_Q^2 \gamma_0} \right) \left. \right\}$ |
| M-ary SQAM | $P_s^{SQAM}(\gamma_0) = \frac{2}{\pi} \frac{1+K}{\gamma_0} \frac{M-1}{9} \left(1 - \frac{1}{\sqrt{M}} \right) \sum_{m=0}^{\infty} \frac{(-1)^m}{m!} \left(\frac{K}{1+\Gamma^2} \right)^m {}_2F_1(-m, -m; 1; \Gamma^2) \quad (14)$ $\times \left[3\pi {}_2F_1 \left(\frac{3}{2}, m+1; 2; -\frac{2(K+1)(M-1)}{3\gamma_0} \right) \right.$ $\left. - \sqrt{2} \left(1 - \frac{1}{\sqrt{M}} \right) F_1 \left(\frac{3}{2}; \frac{1}{2}, m+1; \frac{5}{2}; \frac{1}{2}, -\frac{(K+1)(M-1)}{3\gamma_0} \right) \right]$ |
| M-ary ASK | $P_s^{ASK}(\gamma_0) = \frac{1+K}{\gamma_0} \sum_{m=0}^{\infty} \frac{(-1)^m}{m!} \left(\frac{K}{1+\Gamma^2} \right)^m {}_2F_1(-m, -m; 1; \Gamma^2) \quad (15)$ $\times \frac{(M^2 - 1)(M - 1)}{6M} {}_2F_1 \left(\frac{3}{2}, m+1; 2; -\frac{(K+1)(M^2 - 1)}{3\gamma_0} \right)$ |
| QPSK | $P_s^{QPSK}(\gamma_0) = \frac{1}{3\pi} \frac{1+K}{\gamma_0} \sum_{m=0}^{\infty} \frac{(-1)^m}{m!} \left(\frac{K}{1+\Gamma^2} \right)^m {}_2F_1(-m, -m; 1; \Gamma^2) \quad (16)$ $\times \left[3\pi {}_2F_1 \left(\frac{3}{2}, m+1; 2; -\frac{2(K+1)}{\gamma_0} \right) - \frac{1}{\sqrt{2}} F_1 \left(\frac{3}{2}; \frac{1}{2}, m+1; \frac{5}{2}; \frac{1}{2}, -\frac{K+1}{\gamma_0} \right) \right]$ |
| BPSK | $P_s^{BPSK}(\gamma_0) = \frac{1+K}{4\gamma_0} \sum_{m=0}^{\infty} \frac{(-1)^m}{m!} \left(\frac{K}{1+\Gamma^2} \right)^m {}_2F_1(-m, -m; 1; \Gamma^2) {}_2F_1 \left(\frac{3}{2}, m+1; 2; -\frac{K+1}{\gamma_0} \right) \quad (17)$ |
| M-ary DPSK | $P_s^{DPSK}(\gamma_0) = \sum_{m=0}^{\infty} \frac{{}_2F_1(-m, -m; 1; \Gamma^2)}{m!} \left(\frac{-K}{1+\Gamma^2} \frac{\gamma_0 \sin^2 \frac{\pi}{M}}{1+K+\gamma_0 \sin^2 \frac{\pi}{M}} \right)^m \quad (18)$ $\times \sum_{p=0}^{\infty} \binom{m+p}{p} \left(\frac{-(K+1) \cos \frac{\pi}{M}}{K+1+\gamma_0 \sin^2 \frac{\pi}{M}} \right)^p \left(\frac{m}{m+p} - \frac{\gamma_0 \sin^2 \frac{\pi}{M}}{1+K+\gamma_0 \sin^2 \frac{\pi}{M}} \right)$ $\times \left(\frac{\Gamma \left[\frac{p+1}{2} \right]}{2\sqrt{\pi} \Gamma \left[\frac{p+2}{2} \right]} - \frac{(-\cos \frac{\pi}{M})^{p+1}}{\pi(p+1)} {}_2F_1 \left(\frac{1}{2}, \frac{p+1}{2}; \frac{p+3}{2}; \cos^2 \frac{\pi}{M} \right) \right)$ |

Table IV: Asymptotic ASEP expressions

| Modulation | ASEP |
|---------------|---|
| M-ary RQAM | $P_s^{RQAM}(\gamma_0) \approx \frac{2(M_I - 1)(M_Q - 1)}{(A_I A_Q M_I M_Q)} \left[\frac{A_Q}{A_I} \left(\tan^{-1}(A_I, A_Q) + \frac{\pi}{2(M_Q - 1)} \right) - \frac{A_I}{A_Q} \left(\tan^{-1}(A_I, A_Q) - \frac{\pi M_I}{2(M_I - 1)} \right) + 1 \right] \frac{K + 1}{\pi \gamma_0} e^{-K} I_0 \left(\frac{2\Gamma K}{\Gamma^2 + 1} \right)$ (19) |
| M-ary SQAM | $P_s^{SQAM}(\gamma_0) \approx \left(1 + \frac{\pi(1 + \sqrt{M})}{2(\sqrt{M} - 1)} \right) \frac{2(\sqrt{M} - 1)^2(M - 1)}{3M} \frac{K + 1}{\pi \gamma_0} e^{-K} I_0 \left(\frac{2\Gamma K}{\Gamma^2 + 1} \right)$ (20) |
| M-ary ASK | $P_s^{ASK}(\gamma_0) \approx \frac{(K + 1)(M - 1)(M^2 - 1)}{6\gamma_0 M} e^{-K} I_0 \left(\frac{2\Gamma K}{\Gamma^2 + 1} \right)$ (21) |
| QPSK | $P_s^{QPSK}(\gamma_0) \approx \left(3 + \frac{2}{\pi} \right) \frac{K + 1}{4\gamma_0} e^{-K} I_0 \left(\frac{2\Gamma K}{\Gamma^2 + 1} \right)$ (22) |
| BPSK | $P_s^{BPSK}(\gamma_0) \approx \frac{K + 1}{4\gamma_0} e^{-K} I_0 \left(\frac{2\Gamma K}{\Gamma^2 + 1} \right)$ (23) |
| M-ary DPSK | $P_s^{DPSK}(\gamma_0) \approx \frac{1}{M} \frac{(K + 1)(M - 1)}{K + 1 + \gamma_0 \sin^2 \frac{\pi}{M}} e^{\frac{-K\gamma_0 \sin^2 \frac{\pi}{M}}{K + 1 + \gamma_0 \sin^2 \frac{\pi}{M}}} I_0 \left(\frac{2\Gamma}{1 + \Gamma^2} \frac{K\gamma_0 \sin^2 \frac{\pi}{M}}{K + 1 + \gamma_0 \sin^2 \frac{\pi}{M}} \right)$ (24) |

2) *M*-ary DPSK: In order to derive the asymptotic M-ary DPSK expression, one can show that in (18) $\sum_{p=0}^{\infty} (\cdot) \sim \left(1 - \frac{1}{M}\right) \frac{1+K}{1+K+\gamma_0 \sin^2 \frac{\pi}{M}}$ when $\gamma_0 \rightarrow \infty$, which can be, according to [8, eq. (23)], reduced to a final form of a M-ary DPSK asymptotic ASEP given by (24) in Table IV.

IV. NUMERICAL RESULTS AND DISCUSSION

In this section, we compared analytical results of the exact and asymptotic analysis conducted in Section III with the results obtained using Monte-Carlo simulation.

A. Exact analysis

In order to verify derived exact ASEP expressions and to investigate the impact of different modulation orders, schemes and fading parameters on error performance in TWDP channels, (13) - (15) and (18) versus average SNR are illustrated in Fig. 1 - Fig. 3, together with the results obtained by the corresponding Monte-Carlo simulations generated using 10^5 samples. An excellent match between analytical and simulated results, for all considered modulation orders *M* and TWDP parameter tuples (K, Γ) , can be observed from all the figures. That validates derived theoretical expressions summarized in Table I and enable us to make conclusions about the behaviour of differently modulated signals in different TWDP fading channels.

Accordingly, the impact of different fading conditions (expressed by different values of a tuple (K, Γ)) on ASEP are illustrated in Fig. 1, for 4x2 RQAM modulation (with $\beta = 1$). From Fig. 1a can be observed that for a fixed value of K , performances degrade with the increasement of Γ , ranging from those obtained in Rician channel with the same K , to those obtained in hyper-Rayleigh channels. From Fig. 1b can also be observed that for a small and moderate values of Γ (e.g. $\Gamma = 0.5$), error probability reduces as K grows. Conversely, Fig. 1c indicates that for a large values of Γ ($\Gamma \rightarrow 1$), error probability increases with the increasement of K , finally becoming worse than the one obtained for Rayleigh channel.

Fig. 1a also reveals benefits of Γ -based parameterization in respect to Δ -based. Namely, by comparing ASEP curves given in Fig. 1a with those given in [25, Fig. 4] (for BPSK), it can be observed that for the same absolute values of parameters Δ and Γ ($\Delta \in \{0, 0.25, 0.5, 1\}$ and $\Gamma \in \{0, 0.25, 0.5, 1\}$), Δ -parameterized ASEP curves are almost indistinguishable when Δ changes its values from 0 to 0.5. On the contrary, Γ -parameterized ASEP curves differ notably, enabling us to clearly observe the impact of the increment of the ratio between specular components on error performances in TWDP channels.

The impact of different ratios between d_I and d_Q within RQAM, i.e. $\beta \in [0.5, 1, 2]$, on ASEP, is illustrated in Fig. 2, which presents ASEPs of 4x2 RQAM for $(K = 10$ and $\Gamma = 0.5)$ and $(K = 10$ and $\Gamma = 1)$. The figure shows that for a considered channel conditions, minimum ASEP is achieved for $\beta = 1$, i.e. when in-phase and quadrature distances are the same.

So, considering the results provided in Fig. 2, Fig. 3 enables us to compare the best case RQAM ASEP obtained for $\beta = 1$, with the results obtained for M-ary SQAM, M-ary ASK and M-ary DPSK for the same values of $M \in \{4, 16, 64\}$ and for different values of a tuple (K, Γ) i.e. $(K = 10$ and $\Gamma = 0.5)$ and $(K = 10$ and $\Gamma = 1)$. Accordingly, Fig. 3a - Fig. 3d reveal superiority of SQAM in respect to generalized RQAM, ASK and DPSK, since it provides minimum ASEP for the same value of SNR. Since the aforesaid can be observed for all considered fading conditions and modulation orders, one can conclude that SQAM modulation has the highest energy efficiency among the others treated, which, together with its high bandwidth efficiency and its implementation simplicity, justifies the widespread applicability of SQAM modulation in highly-demanding 5G networks.

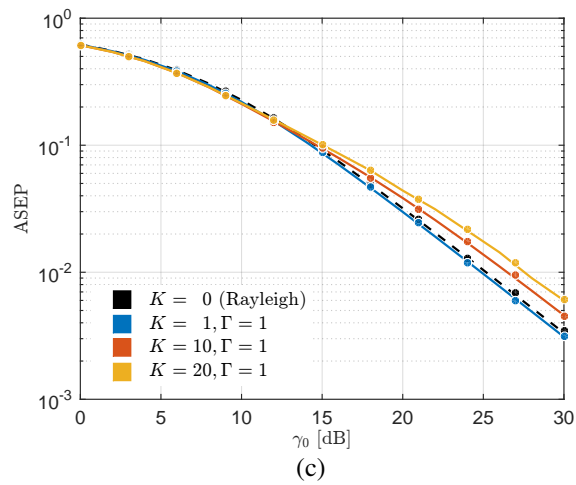
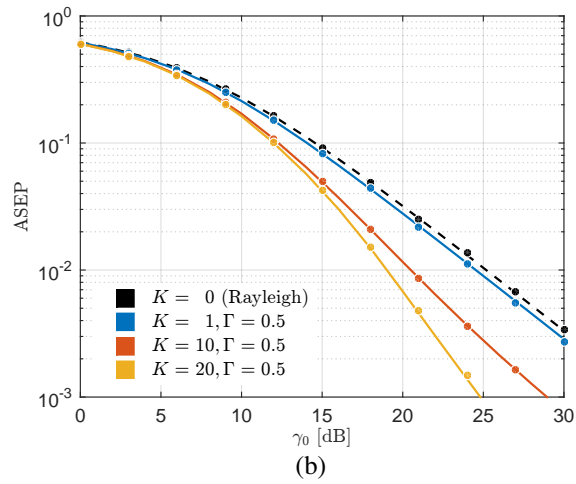
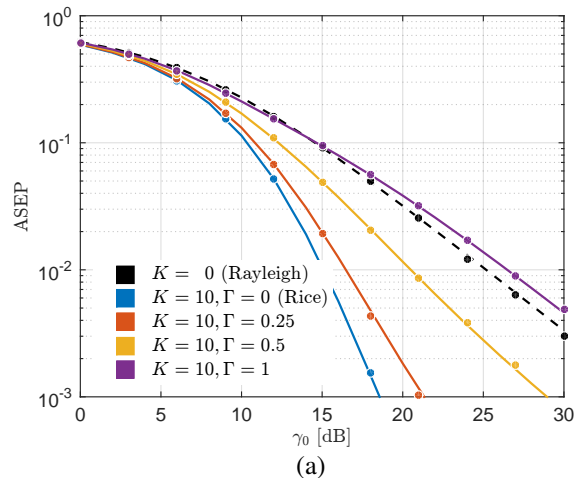


Figure 1: Analytical (solid line) and simulated (dots) ASEP vs. average symbol SNR for 4x2 RQAM modulation

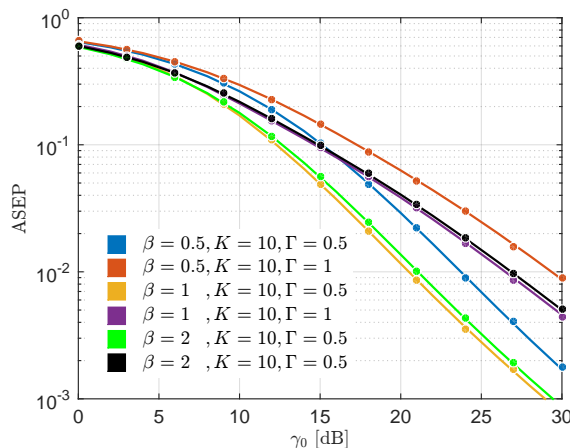


Figure 2: Analytical (solid line) and simulated (dots) ASEP vs. average symbol SNR for 4x2 RQAM modulation, for different combinations of (K, Γ) and different values of β

B. Asymptotic analysis

At the end of this Section, we also provide numerical results to validate performed asymptotic error performance analysis, with its results summarized in Table IV. Accordingly, Fig. 4 illustrates the existing analytical ASEP expressions (i.e. (13), (14) and (18)) obtained for 4x2-RQAM, 16-SQAM and 8DPSK and $K \in [5, 10]$ and $\Gamma \in [0, 0.5, 1]$. Additionally, analytical results and those obtained from asymptotic closed-form expressions given by (19), (20) and (24) are also presented for considered modulation orders and values of a tuple (K, Γ) , enabling us to compare the exact and the asymptotic expressions in different propagation scenarios, ranging from better-than-Rice to worse-than-Rayleigh fading conditions.

From Fig. 4 can be observed that the derived asymptotic results show great agreement with analytical ASEP curves in the high SNR region (i.e. for $\text{SNR} > 30$ dB). It also can be noticed that the results are the worst in terms of SNR lower bound for channel conditions which can be described also by using Rician distribution (i.e. for $\Gamma = 0$), while for conditions which can only be described by TWDP distribution, asymptotic and the exact ASEP expressions remarkably agree even for considerably smaller values of SNR (typically greater than $\text{SNR} > 20$ dB). Accordingly, derived asymptotic ASEP expressions summarized in Table IV can be effectively utilized to provide the explicit insights into the achievable error rate performance of RQAM, SQAM and DPSK modulated signal over the TWDP fading channels for high SNR, for varieties of

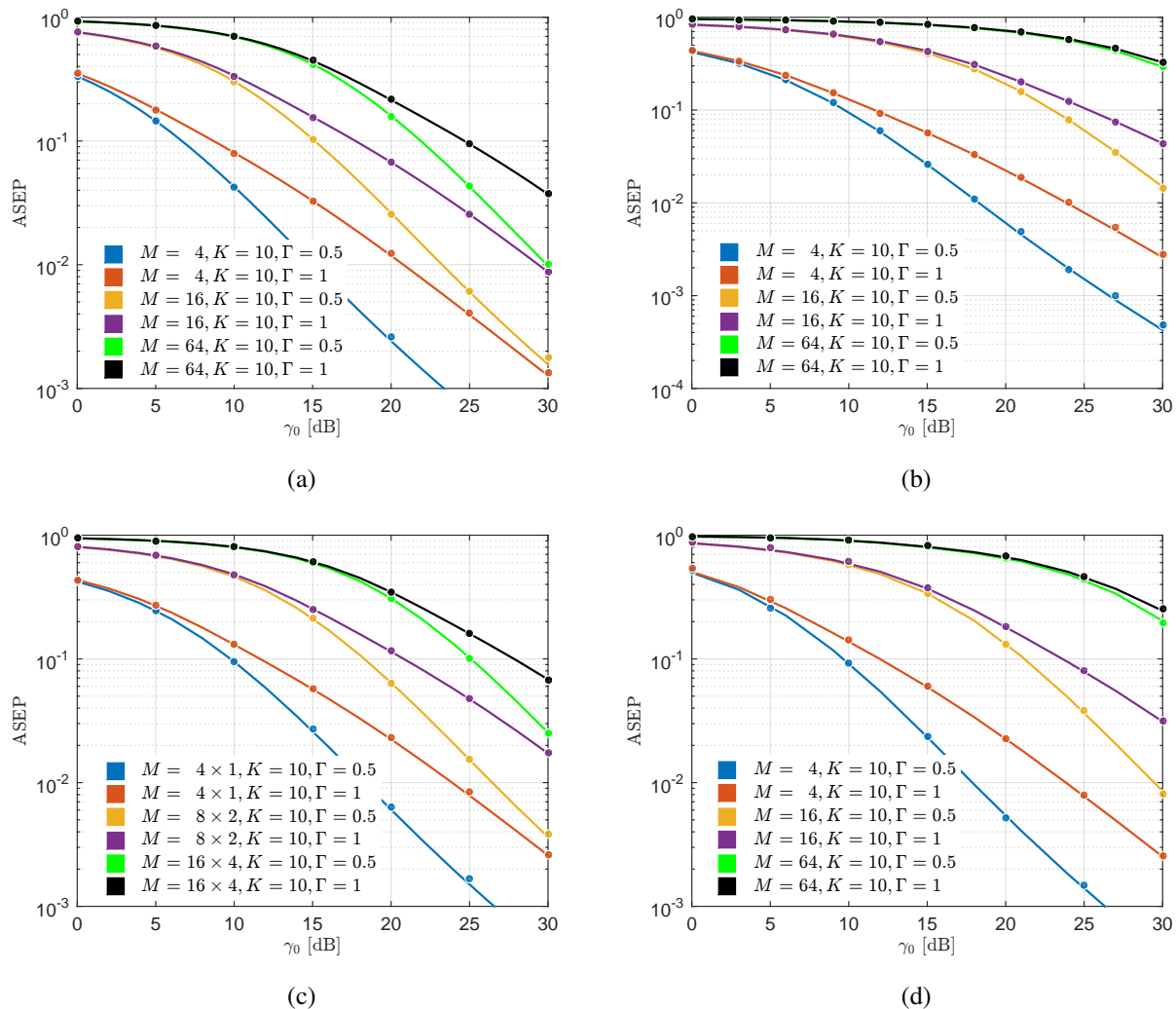


Figure 3: Analytical (solid line) and simulated (dots) ASEP vs. average symbol SNR for (a) M-ary SQAM (b) M-ary ASK, (c) M-ary RQAM and (d) M-ary DPSK modulation

modulation orders and fading conditions.

V. CONCLUSION

Despite the prevalence of TWDP model in description of a small-scale fading effects in mmWave band and cavity sensor networks, the exact ASEP expressions are to date provided only for M-ary PSK and M-ary FSK. Accordingly, in this paper, the exact and high-SNR asymptotic ASEP expression are derived for M-ary RQAM and M-ary SQAM with coherent detection, as well as for differential detected M-ary PKS modulation, thus closing the gap by providing the

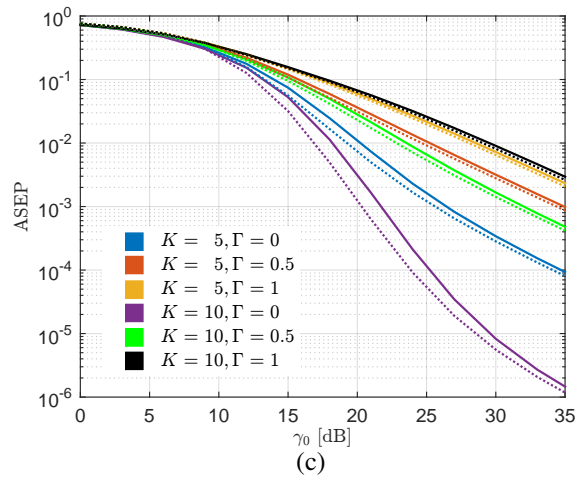
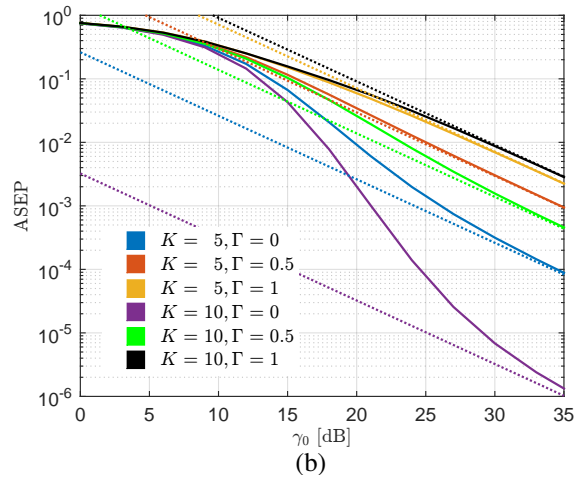
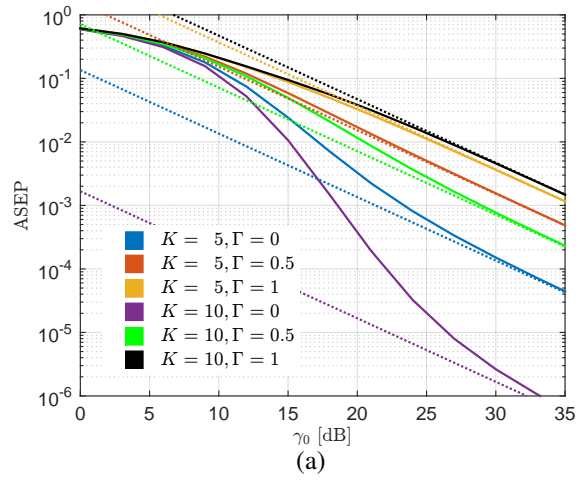


Figure 4: Asymptotic (dotted line) and the exact (solid line) ASEP vs. average symbol SNR for (a) 4x2-RQAM, (b) 16-SQAM and (c) 8DPSK modulations

exact ASEP expressions for the most popular modulations with the single-antenna reception. Analytical results are shown to be in perfect accordance with simulated results, thus providing the appropriate tool for accurate analytical evaluation of error performances in TWDP fading channels.

ACKNOWLEDGMENT

The authors would like to thank Prof. Ivo Kostić for many valuable discussions and advice.

REFERENCES

- [1] G. D. Durgin, T. S. Rappaport, and D. A. de Wolf, "New analytical models and probability density functions for fading in wireless communications," *IEEE Transactions on Communications*, vol. 50, no. 6, pp. 1005–1015, 2002.
- [2] E. Zöchmann, S. Caban, C. F. Mecklenbräuker, S. Pratschner, M. Lerch, S. Schwarz, and M. Rupp, "Better than Rician: Modelling millimetre wave channels as two-wave with diffuse power," *EURASIP Journal on Wireless Communications and Networking*, vol. 2019, no. 1, Jan. 2019.
- [3] E. Zöchmann, M. Hofer, M. Lerch, S. Pratschner, L. Bernadó, J. Blumenstein, S. Caban, S. Sangodoyin, H. Groll, T. Zemen, A. Prokeš, M. Rupp, A. F. Molisch, and C. F. Mecklenbräuker, "Position-specific statistics of 60 GHz vehicular channels during overtaking," *IEEE Access*, vol. 7, pp. 14 216–14 232, 2019.
- [4] T. Mavridis, L. Petrillo, J. Sarrazin, A. Benlarbi-Delaï, and P. De Doncker, "Near-body shadowing analysis at 60 GHz," *IEEE Transactions on Antennas and Propagation*, vol. 63, no. 10, pp. 4505–4511, 2015.
- [5] J. Frolik, "A case for considering hyper-Rayleigh fading channels," *IEEE Transactions on Wireless Communications*, vol. 6, no. 4, pp. 1235–1239, 2007.
- [6] —, "On appropriate models for characterizing hyper-Rayleigh fading," *IEEE Transactions on Wireless Communications*, vol. 7, no. 12, pp. 5202–5207, 2008.
- [7] M. Rao, F. J. Lopez-Martinez, M. Alouini, and A. Goldsmith, "MGF approach to the analysis of generalized two-ray fading models," *IEEE Transactions on Wireless Communications*, vol. 14, no. 5, pp. 2548–2561, 2015.
- [8] A. Maric, P. Njemcevic, and E. Kaljic, "An alternative statistical characterization of TWDP fading model," May, 2021, submitted to *IEEE Trans. on Wir. Comm.* [Online]. Available: <https://arxiv.org/abs/2106.07977>
- [9] S. H. Oh, K. H. Li, and W. S. Lee, "Performance of BPSK pre-detection MRC systems over two-wave with diffuse power fading channels," *IEEE Transactions on Wireless Communications*, vol. 6, no. 8, pp. 2772–2775, 2007.
- [10] S. H. Oh and K. H. Li, "BER performance of BPSK receivers over two-wave with diffuse power fading channels," *IEEE Transactions on Wireless Communications*, vol. 4, no. 4, pp. 1448–1454, 2005.
- [11] R. Subadar and A. D. Singh, "Performance of SC receiver over TWDP fading channels," *IEEE Wireless Communications Letters*, vol. 2, no. 3, pp. 267–270, 2013.
- [12] P. Das and R. Subadara, "Performance of M-EGC receiver over TWDP fading channels," *IET Communications*, vol. 11, no. 12, pp. 1853–1856, 2017.
- [13] R. Subadara and A. D. Singh, "Performance of M-MRC receivers over TWDP fading channels," *International Journal of Electronics and Communications*, vol. 68, no. 6, pp. 569–572, 2014.
- [14] S. Singh and V. Kansal, "Performance of M-ary PSK over TWDP fading channels," *International Journal of Electronics Letters*, vol. 4, no. 4, pp. 433–437, 2016.

- [15] B. S. Tan, K. H. Li, and K. C. Teh, "Symbol-error rate of selection combining over two-wave with diffuse power fading," in *2011 5th International Conference on Signal Processing and Communication Systems (ICSPCS)*, 2011.
- [16] D. Dixit and P. R. Sahu, "Performance of QAM signaling over TWDP fading channels," *IEEE Transactions on Wireless Communications*, vol. 12, no. 4, pp. 1794–1799, 2013.
- [17] H. A. Suraweera, W. S. Lee, and S. H. Oh, "Performance analysis of QAM in a two-wave with diffuse power fading environment," *IEEE Communications Letters*, vol. 12, no. 2, pp. 109–111, 2008.
- [18] P. Das and R. Subadar, "Performance analysis of QAM for M-SC receiver over TWDP fading channels," *International Journal of Electronics Letters*, vol. 6, no. 4, pp. 438–444, 2018. [Online]. Available: <https://doi.org/10.1080/21681724.2017.1382000>
- [19] Y. Lu and N. Yang, "Symbol error rate of decode-and-forward relaying in two-wave with diffuse power fading channels," *IEEE Transactions on Wireless Communications*, vol. 11, no. 10, pp. 3412–3417, 2012.
- [20] S. Haghani, "Average BER of BFSK with postdetection switch-and-stay combining in TWDP fading," in *2011 IEEE Vehicular Technology Conference (VTC Fall)*, 2011.
- [21] W. S. Lee and S. H. Oh, "Performance of dual switch-and-stay diversity NCFSK systems over two-wave with diffuse power fading channels," in *2007 6th International Conference on Information, Communications & Signal Processing*, 2007.
- [22] W. S. Lee, "Performance of postdetection EGC NCFSK and DPSK systems over two-wave with diffuse power fading channels," in *2007 International Symposium on Communications and Information Technologies*, 2007.
- [23] S. Haghani and H. Dashtestani, "BER of noncoherent MFSK with postdetection switch-and-stay combining in TWDP fading," in *2012 IEEE Vehicular Technology Conference (VTC Fall)*, 2012.
- [24] J. P. Peña-Martín, J. M. Romero-Jerez, and F. J. Lopez-Martinez, "Generalized MGF of the two-wave with diffuse power fading model with applications," *IEEE Transactions on Vehicular Technology*, vol. 67, no. 6, pp. 5525–5529, 2018.
- [25] M. Rao, F. J. Lopez-Martinez, and A. Goldsmith, "Statistics and system performance metrics for the two wave with diffuse power fading model," in *2014 48th Annual Conference on Information Sciences and Systems (CISS)*, 2014.
- [26] I. M. Kostic, "Envelope probability density function of the sum of signal, noise and interference," *Electronics Letters*, vol. 14, no. 15, pp. 490–491, 1978.
- [27] P. Njemcevic, A. Maric, and E. Kaljic, "Moment-based parameter estimation for Γ -parameterized TWDP model," June, 2021, submitted to *IEEE Trans. on Wir. Comm.* [Online]. Available: <https://arxiv.org/abs/2106.09969>
- [28] Y. Lu and N. Yang, "Symbol error probability of QAM with MRC diversity in two-wave with diffuse power fading channels," *IEEE Communications Letters*, vol. 15, no. 1, pp. 10–12, 2011.
- [29] D. Kim, H. Lee, and J. Kang, "Comprehensive analysis of the impact of TWDP fading on the achievable error rate performance of BPSK signaling," *IEICE Transactions on Communications*, vol. E101.B, no. 2, pp. 500–507, 2018.